Hindawi Publishing Corporation
Advances in Optical Technologies
Volume 2012, Article ID 814745, 6 pages
doi:10.1155/2012/814745

Research Article

Optical Properties of Afterglow Nanoparticles $Sr_2MgSi_2O_7$: Eu^{2+}, Dy^{3+} Capped with Polyethylene Glycol

Fumitaka Yoshimura, Mika Ishizaki, Fumihiro Wakai, Masahiko Hara, Osamu Odawara, and Hiroyuki Wada

Tokyo Institute of Technology, 4259 Nagatsuda, Midori-ku, Yokohama 226-8503, Japan

Correspondence should be addressed to Hiroyuki Wada, wada.h.ac@m.titech.ac.jp

Received 24 March 2011; Accepted 18 May 2011

Academic Editor: Siu-Fung Yu

The optical properties of afterglow nanoparticles were successfully improved by the addition of polyethylene glycol (PEG) to an afterglow colloidal solution. Afterglow nanoparticles—$Sr_2MgSi_2O_7$: Eu^{2+}, Dy^{3+}—were prepared by laser ablation in liquid. The quantum yields and the decay curves were measured by a fluorescence spectrophotometer. An increase in the amount of PEG added to the solution increased the quantum yield of the nanoparticles and improved the afterglow property in the initial portion of the decay curve. However, the afterglow property did not change after a substantial amount of time had passed. The afterglow nanoparticles were capped with PEG molecules, and surface defects of the nanoparticles were passivated, which decreased the optical properties.

1. Introduction

In the past several years, there has been increasing interest in nanoparticles due to their unique properties and various applications in research fields, such as biotechnology and electronics. There are many methods available to create nanoparticles, such as gas-phase preparation [1, 2] and liquid-phase preparation [3, 4]. One of the liquid-phase preparation methods is laser ablation in liquid, which has recently been studied extensively [5–9]. While laser ablation in the gas phase, such as under vacuum and in argon, has been used for various research purposes [10], laser ablation, in liquid, has been investigated more recently [11, 12]. In the case of laser ablation in liquid, the target material in the liquid is irradiated with a focused, pulsed laser beam without using a chamber. Precipitation methods, such as the sol-gel method, are well known as synthesis methods for nanoparticles. However, it is difficult to prepare multielement nanoparticles with these techniques. In the case of the trioctylphosphine oxide (TOPO) method [4], the popular synthesis method used to create quantum dots, coating materials are limited to specific surfactants, such as TOPO. In contrast, in the case of laser ablation in liquid, multielement nanoparticles can be easily prepared. By using laser ablation in liquid, surfactant-free nanoparticles can be prepared, and/or a desirable coating material can be selected.

We prepared functionalized multielement nanoparticles with afterglow properties by using laser ablation in liquid [13]. Afterglow is a promising optical property for various fields because of the long emitting time (e.g., several hours) after the excitation is blocked. In the case of normal fluorescence, materials emit during excitation but do not emit after the excitation is blocked. On the contrary, in the case of afterglow, materials emit both during excitation and after the excitation is blocked. The long-afterglow material $SrAl_2O_4$: Eu^{2+}, Dy^{3+} was discovered by Matuzawa in 1996 [14]. However, it is water soluble. $Sr_2MgSi_2O_7$: Eu^{2+}, Dy^{3+}, a water-insoluble afterglow material, was recently proposed by numerous research groups [15–18]. If these afterglow materials can be nanosized, they would be very useful in many fields. One example is as a marker for bioimaging. This system would resolve the existing problem of autofluorescence in which the excitation of markers also excites fluorescent materials, such as NADH and tryptophan,

which exist in living cells. Ideally, only the marker would emit when afterglow nanoparticles were used as markers, and the excitation light was blocked.

Capping nanoparticles with polymer molecules has been studied previously. The advantages of capping are as follows: (1) the passivation of surface defects, which decreases the nonradiative recombination center and increases fluorescence intensity [19–21]; (2) the aggregation inhibition of nanoparticles by steric rather than electrostatic effects; (3) the ability to utilize nanoparticles for a drug delivery system (DDS) because of the improvement in immunoaffinity, especially in the case of capping nanoparticles with polyethylene glycol (PEG).

In this study, the optical properties of afterglow nanoparticles capped with PEG were investigated. We prepared the afterglow nanoparticles by laser ablation in liquid. However, the reduction in particle size decreased the optical properties. The probability of an increase in the optical properties of nanoparticles was examined by the addition of PEG to the colloidal liquid.

2. Experimental Methods

Figure 1 shows the equipment used for laser ablation in liquid. The target in DI water in a cell was irradiated with a focused, pulsed laser beam. The laser was a third-harmonic generation pulsed laser (JDS Uniphase Co., Model 210, THG, wavelength: 355 nm, pulse width: 50 ns, energy: 0.5 mJ/pulse, average energy density: 0.85 J/cm^2). The target material $Sr_2MgSi_2O_7$: Eu^{2+}, Dy^{3+}, which has afterglow properties, was purchased from the Mitsubishi Chemical Corporation. The target was fabricated by spark plasma sintering (SPS, SPS Syntex Inc., SPS-515S, pressure: 50 MPa, electric current: 540 A, voltage: 2.4 V, temperature: 1100°C, sintering time: 10 min, atmosphere: Ar).

The synthesized nanoparticles were identified by an X-ray diffractometer (XRD, PANalytical B.V. X'pert-PRO-MRD). The sample powder was obtained by centrifugation. The optical properties (fluorescence and afterglow) were measured by a fluorescence spectrophotometer (Hitachi High-Technologies Co., F-7000).

3. Results and Discussion

Figure 2 shows the optical properties of the target material. The PL spectrum (Figure 2(a)) with an excitation wavelength of 276 nm had a main, broad, blue-green peak at 466 nm, which was attributed to the f-d transitions of Eu^{2+} ions [22]. The strong peak at approximately 555 nm represents the second-order scattering of the excitation light. The PLE spectrum (Figure 2(b)) with an emission wavelength of 466 nm has 2 peaks at 275 nm and 361 nm. These peaks are due to defect levels of the host material; therefore, the peak shape is changed by the synthesis method [22]. The increase in absorbance less than 237 nm was probably caused by band-edge absorption of the host material, whose bandgap was 7.1 eV (175 nm) [23]. The strong peak at 232 nm was the second-order scattering of a 466-nm excitation wavelength.

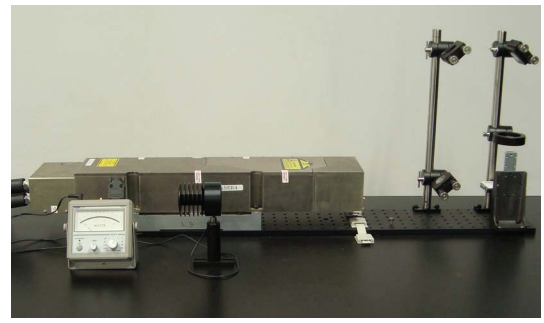

Figure 1: Equipment for laser ablation in liquid.

Figure 3 shows an XRD pattern of the synthesized nanoparticles prepared in DI water with an average energy density of 0.85 J/cm^2. These data corresponded to the powder diffraction file data for $Sr_2MgSi_2O_7$ (PDF-4 10753217), which was the target. Strontium carbonate was formed as a byproduct. The target material might react with carbonate, which is formed by the dissolution of carbon dioxide in DI water.

Figure 4 shows PL spectra of the synthesized nanoparticles with the addition of PEG. The concentration of PEG was varied (a: 1 mM, b: 0.1 mM, c: 0 mM). The shape and peak wavelength of each spectrum were almost the same as those of the target material. In general, the fluorescence of Eu^{2+} is due to the transition from the $4f^6 5d^1$ level, which causes a broad emission [24]. On the contrary, the fluorescence of Eu^{3+}, whose 4f electrons are shielded from external electric fields by the outer 5s and 5p electrons, is sharp and appears at approximately 600 nm [24]. The wavelength of the fluorescence spectra of the f-d transitions of Eu^{2+} is sensitive to the crystal field, whereas that of the f-f transitions of Eu^{3+} is not affected because the 4f electrons are shielded by 5s and 5d electrons [24]. The PL spectra of nanoparticles prepared by laser ablation in liquid were the same as those of the target. Therefore, the luminescent center, Eu^{2+}, and the host material were not transformed by the laser ablation in liquid and the addition of PEG, although Eu^{2+} was likely to be easily oxidized.

Figure 5 shows the quantum yield of nanoparticles as a function of the PEG concentration. A dotted line was added as a guide. An increase in the PEG concentration increased the quantum yield of the afterglow nanoparticles, although the increase rate was slightly low at a high PEG concentration. The reason for this increase would be as follows: PEG molecules would adhere to the nanoparticles, as shown in Figure 6, and passivate defect levels, which reduced the fluorescence intensity. The quantum yield was saturated at a high PEG concentration because passivation of the whole surface of the nanoparticle would be covered with the addition of enough PEG. In general, killer defects, which create surface levels, exist on the surface of particles. The reduction of particle size increases the specific surface area of the particle. Therefore, the florescence intensity and the quantum yield are decreased in the case of nanoparticles. There were many reports that passivation of fluorescent nanoparticles by polymers increased the fluorescence

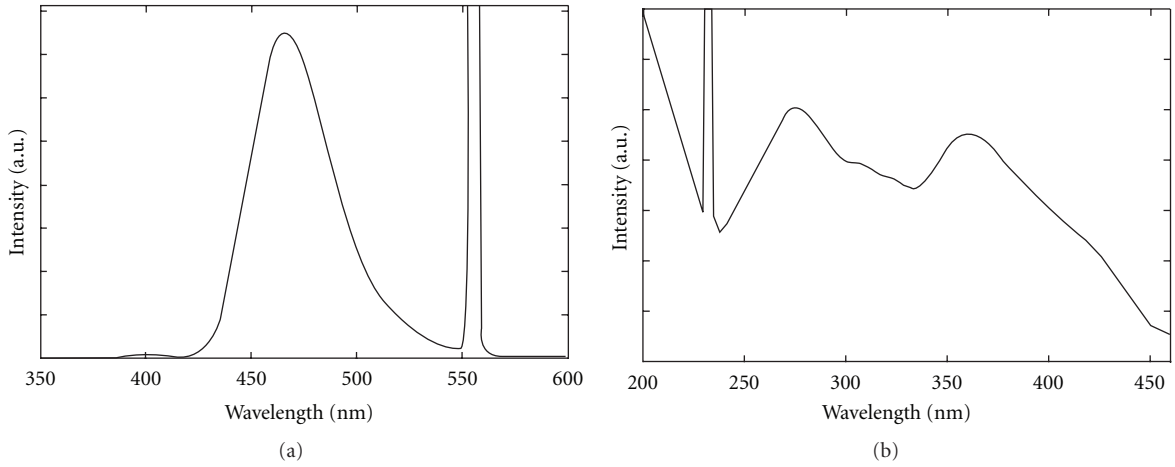

Figure 2: Optical properties of $Sr_2MgSi_2O_7$: Eu^{2+}, Dy^{3+}. (a) Photoluminescence spectrum (excitation wavelength: 276 nm). (b) Photoluminescence excitation spectrum (emission wavelength: 466 nm).

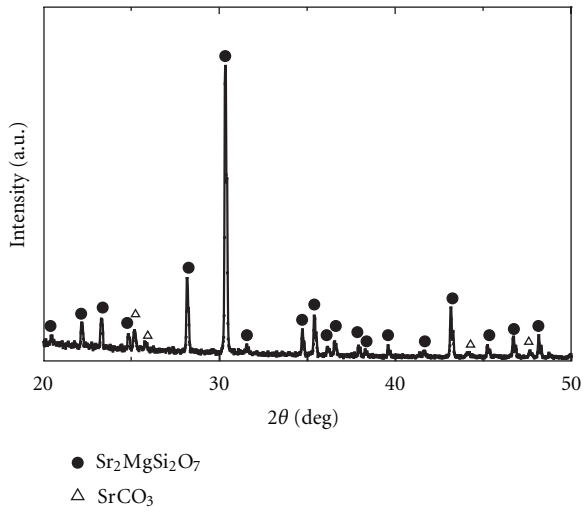

Figure 3: XRD pattern of the synthesized nanoparticles prepared by laser ablation in liquid (DI water, average energy density: 0.85 J/cm^2).

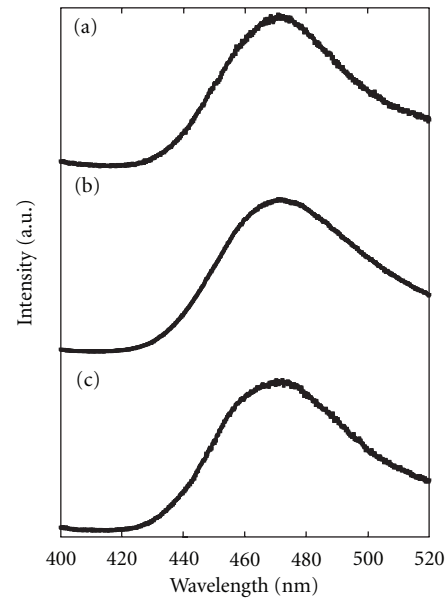

Figure 4: PL spectra of the synthesized nanoparticles with the addition of PEG. PEG concentration: (a) 1 mM, (b) 0.1 mM, and (c) 0 mM.

intensity[19–21]. Capping nanoparticles with PEG is also important for minimizing the nonspecific adsorption of proteins related to the immune system [25, 26]. Therefore, PEG-capped nanoparticles are useful for bioimaging and drug delivery system (DDS).

Figure 7 shows decay curves of afterglow nanoparticles at each PEG concentration. Afterglow is caused by the recombination of the trapped carriers [14, 27–31]. For example, trapped holes migrate to the valence band using the thermal energy available at room temperature. These holes result in luminescence through the radiative transition of recombination between electrons and holes. In the case of $SrAl_2O_4$: Eu^{2+}, Dy^{3+}, it has been suggested that holes are trapped at the energy level of Dy^{3+} ions [14]. In the case where the trapped carriers are electrons, equation (1) is applied to the decay curve. This formula can also be applied in the case of holes if the captured cross sections of the traps and the luminescent centers are almost the same [32]:

$$I_{(t)} = \frac{I_0}{(1+\gamma t)^n}, \tag{1}$$

$$\gamma = \frac{N}{an_t}, \tag{2}$$

where $I(t)$ is the afterglow intensity, I_0 is the initial value, t is time, N is the trap concentration, a is the probability that a trapped carrier will be thermally led into the band

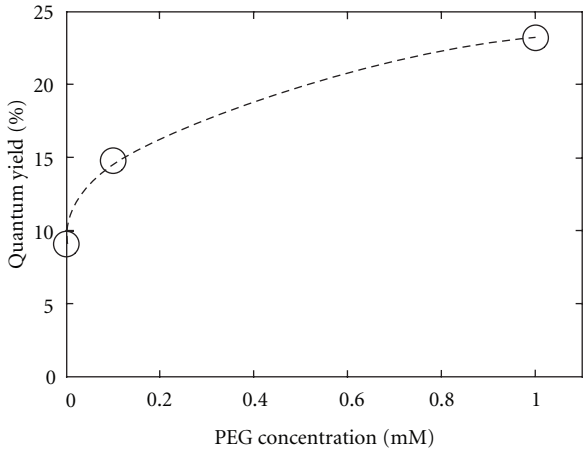

Figure 5: Quantum yield of the nanoparticles as a function of the PEG concentration.

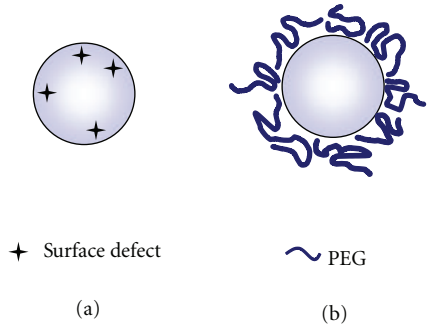

Figure 6: Schematic of an afterglow nanoparticle and of PEG molecules. (a) An afterglow nanoparticle without the addition of PEG. (b) An afterglow nanoparticle capped with PEG molecules at a high PEG concentration.

(given below by (3)), n_t is the number of carriers per unit volume in the trap level, and n is approximately 0.5–2

$$a = s \exp\left(-\frac{E_t}{kT}\right), \tag{3}$$

where s is the frequency factor, E_t is the energy between the conduction band and the trap level, k is the Boltzmann constant, and T is temperature. If t is much less than $1/\gamma$ (the initial period), γ is the dominant parameter compared with n. On the contrary, if t is much greater than $1/\gamma$ (the period after a substantial amount of time has passed), n is the dominant parameter. The values of n and γ can be obtained by the curve fitting of afterglow properties shown in Figure 7. The values of γ at each PEG concentration were as follows: 0.194 ± 0.006 at 1 mM, 0.394 ± 0.019 at 0.1 mM, and 0.604 ± 0.030 at 0 mM, respectively. Because these afterglow properties of nanoparticles in Figure 7 depended on the slopes in the initial period, the values of γ were important to identify the differences in the data. Figure 8 shows the value of γ as a function of the PEG concentration. A dotted line was added as a guide. Addition of PEG significantly reduced the value of γ. A small γ value indicates a significant improvement in the afterglow properties, as shown in (1).

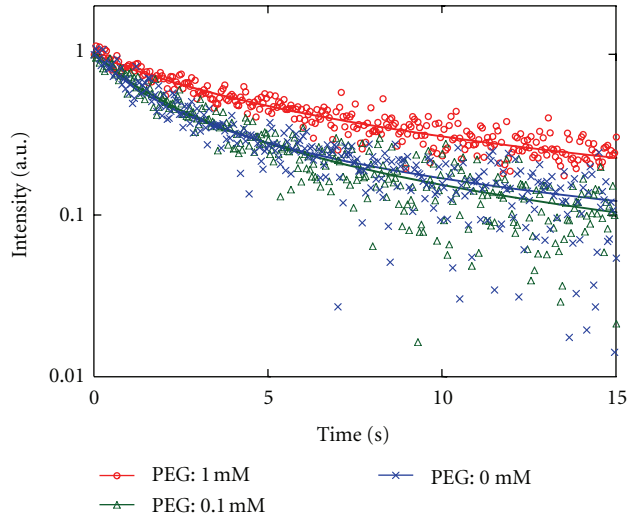

Figure 7: Decay curves of afterglow nanoparticles at each PEG concentration.

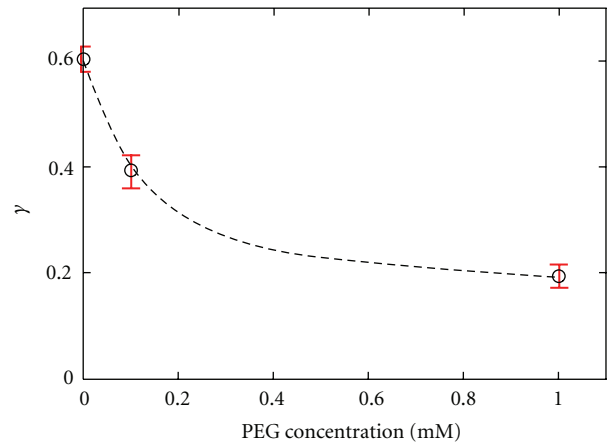

Figure 8: Value of γ as a function of the PEG concentration.

The values of n were almost the same at each PEG concentration. As indicated in the introduction, functionalized fluorescent nanoparticles, such as afterglow nanoparticles, are a promising type of material in various fields. However, as mentioned above, a reduction in the particle size decreases the afterglow properties. The reason for this is as follows: a reduction in the particle size increases the specific surface area of the particles. The increased specific surface area leads to the nonradiative transition of surface defects through the energy levels and to the vibration of water molecules, which decreases the afterglow property. The addition of PEG to the solution in which the nanoparticles were dispersed caused capping nanoparticles [33, 34]. Surface passivation by polymer coating would be effective to prevent such a reduction of afterglow properties [19–21]. In this study, the addition of PEG increased the quantum yield, as shown in Figure 5. An increase in the PEG concentration increased the afterglow property, especially in the initial period shown in Figure 7, although the property had not changed significantly after

a substantial amount of time had passed. We concluded that this improvement was due to the coating effect of PEG.

4. Conclusions

The addition of PEG to afterglow nanoparticle solutions prepared by laser ablation in liquid increased the quantum yield. PEG addition also improved the afterglow property of $Sr_2MgSi_2O_7$: Eu^{2+}, Dy^{3+} nanoparticles in the initial period. The afterglow property was not improved after a substantial amount of time had passed. Because the specific surface area of nanoparticles is large, nanoparticles have many surface defects, which decrease optical properties, such as photoluminescence and afterglow. In this study, these surface defects on afterglow nanoparticles were passivated by PEG molecules, and the optical properties improved. Improvement of the afterglow property is important for a wide range of applications.

Acknowledgments

The authors wish to thank Mr. H. Iida and Mr. Y. Suzuki of the Center for Advanced Materials Analysis (Tokyo Institute of Technology) for the XRD measurements.

References

[1] E. O. Knutson and K. T. Whitby, "Aerosol classification by electric mobility: apparatus, theory, and applications," *Journal of Aerosol Science*, vol. 6, no. 6, pp. 443–451, 1975.

[2] R. G. Osifchin, W. J. Mahoney, J. D. Bielefeld, R. P. Andres, J. I. Henderson, and C. P. Kubiak, "Synthesis of a quantum dot superlattice using molecularly linked metal clusters," *Superlattices and Microstructures*, vol. 18, no. 4, p. 283, 1995.

[3] J. R. Darwent and G. Porter, "Photochemical hydrogen production using cadmium sulphide suspensions in aerated water," *Journal of the Chemical Society, Chemical Communications*, no. 4, pp. 145–146, 1981.

[4] C. B. Murray, D. J. Norris, and M. G. Bawendi, "Synthesis and characterization of nearly monodisperse CdE (E = S, Se, Te) semiconductor nanocrystallites," *Journal of the American Chemical Society*, vol. 115, no. 19, pp. 8706–8715, 1993.

[5] F. Mafuné, J. Y. Kohno, Y. Takeda, T. Kondow, and H. Sawabe, "Structure and stability of silver nanoparticles in aqueous solution produced by laser ablation," *The Journal of Physical Chemistry B*, vol. 104, no. 35, pp. 8336–8337, 2000.

[6] Y. Tamaki, T. Asahi, and H. Masuhara, "Tailoring nanoparticles of aromatic and dye molecules by excimer laser irradiation," *Applied Surface Science*, vol. 168, no. 1–4, pp. 85–88, 2000.

[7] T. Tsuji, K. Iryo, N. Watanabe, and M. Tsuji, "Preparation of silver nanoparticles by laser ablation in solution: influence of laser wavelength on particle size," *Applied Surface Science*, vol. 202, no. 1-2, pp. 80–85, 2002.

[8] C. Liang, Y. Shimizu, T. Sasaki, and N. Koshizaki, "Synthesis, characterization, and phase stability of ultrafine TiO_2 nanoparticles by pulsed laser ablation in liquid media," *Journal of Materials Research*, vol. 19, no. 5, pp. 1551–1557, 2004.

[9] K. Sasaki and N. Takada, "Liquid-phase laser ablation," *Pure and Applied Chemistry*, vol. 82, no. 6, pp. 1317–1327, 2010.

[10] F. Brech and L. Cross, "Optical micromission stimulated by a ruby maser," *Applied Spectroscopy*, vol. 16, no. 2, p. 59, 1962.

[11] J. Neddersen, G. Chumanov, and T. Cotton, "Laser ablation of metals: a new method for preparing SERS active colloids," *Applied Spectroscopy*, vol. 47, no. 12, pp. 1959–1964, 1993.

[12] A. Fojtik and A. Henglein, "Laser ablation of films and suspended particles in a solvent: formation of cluster and colloid solutions," *Berichte der Bunsen-Gesellschaft. Physical Chemistry, Chemical Physics*, vol. 97, no. 2, pp. 252–254, 1993.

[13] F. Yoshimura, K. Nakamura, F. Wakai et al., "Preparation of long-afterglow colloidal solution of $Sr_2MgSi_2O_7$: Eu^{2+}, Dy^{3+} by laser ablation in liquid," *Applied Surface Science*, vol. 257, no. 6, pp. 2170–2175, 2011.

[14] T. Matsuzawa, Y. Aoki, N. Takeuchi, and Y. Murayama, "A new long phosphorescent phosphor with high brightness, $Sr_2MgSi_2O_4$: Eu^{2+}, Dy^{3+}," *Journal of the Electrochemical Society*, vol. 143, no. 8, pp. 2670–2673, 1996.

[15] N. Kodama, T. Takahashi, M. Yamaga, Y. Tanii, J. Qiu, and K. Hirao, "Long-lasting phosphorescence in Ce^{3+}-doped $Ca_2Al_2SiO_7$ and $CaYAl_3O_7$ crystals," *Applied Physics Letters*, vol. 75, no. 12, pp. 1715–1717, 1999.

[16] Q. Fei, C. Chang, and D. Mao, "Luminescent properties of $Sr_2MgSi_2O_7$ and $Ca_2MgSi_2O_7$ long lasting phosphors activated by Eu^{2+}, Dy^{3+}," *Journal of Alloys and Compounds*, vol. 390, no. 1-2, pp. 133–137, 2005.

[17] Y. Chen, B. Liu, M. Kirm et al., "Luminescent properties of blue-emitting long afterglow phosphors $Sr_{2-x}Ca_xMgSi_2O_7$: Eu^{2+}, Dy^{3+} (x = 0, 1)," *Journal of Luminescence*, vol. 118, no. 1, pp. 70–78, 2006.

[18] A. R. Mirhabibi, F. Moztarzadeh, A. A. Bazazi, M. Solati, A. Maghsoudipour, and M. H. Sarrafi, "Studies of luminescence property of long afterglow Eu^{2+}, Dy^{3+} activated $Sr_2MgSi_2O_7$ phosphor," *Pigment and Resin Technology*, vol. 33, no. 4, pp. 220–225, 2004.

[19] J. I. Pankove, *Optical Processes in Semiconductors*, Dover, New York, NY, USA, 1971.

[20] O. I. Mićić, J. Sprague, Z. Lu, and A. J. Nozik, "Highly efficient band-edge emission from InP quantum dots," *Applied Physics Letters*, vol. 68, no. 22, pp. 3150–3152, 1996.

[21] M. Kuno, J. K. Lee, B. O. Dabbousi, F. V. Mikulec, and M. G. Bawendi, "The band edge luminescence of surface modified CdSe nanocrystallites: probing the luminescing state," *Journal of Chemical Physics*, vol. 106, no. 23, pp. 9869–9882, 1997.

[22] F. Song, C. Donghua, and Y. Yuan, "Synthesis of $Sr_2MgSi_2O_7$: Eu, Dy and $Sr_2MgSi_2O_7$: Eu, Dy, Nd by a modified solid-state reaction and their luminescent properties," *Journal of Alloys and Compounds*, vol. 458, no. 1-2, pp. 564–568, 2008.

[23] J. Hölsä, M. Kirm, T. Laamanen, M. Lastusaari, J. Niittykoski, and P. Novák, "Electronic structure of the $Sr_2MgSi_2O_7$: Eu^{2+} persistent luminescence material," *Journal of Luminescence*, vol. 129, no. 12, pp. 1560–1563, 2009.

[24] T. Kano, "Luminescence center of rare-earth ions," in *Phosphor Handbook*, W. M. Yen, S. Shionoya, and H. Yamamoto, Eds., chapyer 3.3, CRC Press, Boca Raton, Fla, USA, 2206.

[25] K. Uchida, H. Otsuka, M. Kaneko, K. Kataoka, and Y. Nagasaki, "A reactive poly(ethylene glycol) layer to achieve specific surface plasmon resonance sensing with a high S/N ratio: the substantial role of a short underbrushed PEG layer in minimizing nonspecific adsorption," *Analytical Chemistry*, vol. 77, no. 4, pp. 1075–1080, 2005.

[26] J. Blümmel, N. Perschmann, D. Aydin et al., "Protein repellent properties of covalently attached PEG coatings on nanostructured SiO_2-based interfaces," *Biomaterials*, vol. 28, no. 32, pp. 4739–4747, 2007.

[27] A. A. Setlur, A. M. Srivastava, H. L. Pham, M. E. Hannah, and U. Happek, "Charge creation, trapping, and long phosphorescence in $Sr_2MgSi_2O_7$: Eu^{2+}, RE^{3+}," *Journal of Applied Physics*, vol. 103, no. 5, Article ID 053513, 2008.

[28] M. Yamaga, Y. Tanii, N. Kodama, T. Takahashi, and M. Honda, "Mechanism of long-lasting phosphorescence process of Ce^{3+}-doped $Ca_2Al_2SiO_7$ melilite crystals," *Physical Review B*, vol. 65, no. 23, Article ID 235108, 2002.

[29] T. Kinoshita, M. Yamazaki, H. Kawazoe, and H. Hosono, "Long lasting phosphorescence and photostimulated luminescence in Tb-ion-activated reduced calcium aluminate glasses," *Journal of Applied Physics*, vol. 86, no. 7, pp. 3729–3733, 1999.

[30] J. Qiu and A. Makishima, "Ultraviolet-radiation-induced structure and long-lasting phosphorescence in Sn^{2+}-Cu^{2+} co-doped silicate glass," *Science and Technology of Advanced Materials*, vol. 4, no. 1, pp. 35–38, 2003.

[31] M. Yamaga and N. Kodama, "Fluorescence of Ce^{3+} in fluorides and long-lasting phosphorescence of Ce^{3+} in oxides," *Journal of Alloys and Compounds*, vol. 408–412, pp. 706–710, 2006.

[32] E. Nakazawa, "Transient characteristics of luminescence," in *Phosphor Handbook*, W. M. Yen, S. Shionoya, and H. Yamamoto, Eds., chapter 2.7, CRC Press, Boca Raton, Fla, USA, 2006.

[33] S. Tachikawa, A. Noguchi, M. Hara, O. Odawara, and H. Wada, *Journal of Ceramic Processing Research*, submitted.

[34] S. Tachikawa, A. Noguchi, M. Hara, O. Odawara, and H. Wada, "Optical properties of ZnO nanoparticles capped with polymers," *Materials*, vol. 4, pp. 1132–1143, 2011.